

SCIENTIFIC AND TECHNICAL SECTION

UDC 539.4

Investigation of Ultrasonic Assisted Friction Stir Spot Welding of Magnesium Alloy to Aluminum Alloy

S. D. Ji,¹ Z. W. Li, L. Ma, Y. M. Yue, and S. S. Gao

Faculty of Aerospace Engineering, Shenyang Aerospace University, Daoyi Development District, Shenyang, China

¹ superjds@163.com

A new welding method: ultrasonic assisted friction stir spot welding (UAFSSW) was put forward in the present study. UAFSSW was successfully applied to weld dissimilar AZ31 Mg alloy and 6061 Al alloy. Results show that for either conventional FSSW or UAFSSW, sound joints are obtained in the configuration of upper Mg alloy and lower Al alloy. Ultrasonic vibration is beneficial to the upward flow of lower aluminum alloy, the increase of the stir zone (SZ) width and the refinement of the grains in the SZ. All cross sections of the Al–Mg joints exhibit the formation of intermetallic compounds (IMC) in the SZ. The crack of the conventional FSSW joint propagates exactly along the interface between the dissimilar materials and presents an inverted “V” morphology. After reaching the highest point of the hook defect, crack of the UAFSSW joint extends to the keyhole, leaving a portion of Mg alloy on the lower sheet. Conventional FSSW joint and UAFSSW joint show different IMC compositions at the faying interface.

Keywords: ultrasonic assisted friction stir spot welding, intermetallic compounds, magnesium alloy, aluminum alloy, fracture position.

Introduction. In the last few decades, as the resource shortage and environment protection problems become severer, weight-saving structures have become a hotspot in industries of aerospace and transportations. Therefore, light materials are being extensively used now [1–3]. As a new variant of friction stir welding (FSW), friction stir spot welding (FSSW) owns advantage of lower energy consumption, smaller distortion, less welding defects and higher joint quality compared to resistance spot welding (RSW) [4]. Being a solid state joining technology, FSSW is more suitable to weld light materials such as aluminum alloys and magnesium alloys [5–8].

Since the invention of FSSW, many investigations about FSSW joints of Al alloy or Mg alloy have been reported [9–15]. Yin et al. [9] performed FSSW on AZ31 aluminum alloy and reported that better failure loads can be attained under conditions of larger bonded width, outward curved hook and smaller hook height. Bozzi et al. [10] found out that the FSSW joint strength was largely determined by the stir zone (SZ) width and the hook defect. Besides, some investigations about FSSW dissimilar Al and Mg alloys have been published. Rao et al. [13] investigated effects of the tool rotating speed on dissimilar AM60B Mg alloy and 6022-T4 Al alloy FSSW joints and studied the intermetallic compounds (IMCs) in the SZ. Furthermore, Sato et al. [15] studied the interfacial microstructure on the lap shear strength of Al alloy to Mg alloy FSSW joint. Lots of important conclusions can be obtained from these studies. However, before successful application of the Al–Mg FSSW joints, plenty of researches need to be done.

Ultrasonic assisted FSW (UAFSW) is a new derivative process of FSW. The ultrasonic vibration can increase the heat input during the welding process and decreases the welding force [16]. In the last few years some researches about UAFSW or ultrasonic assisted FSSW (UAFSSW) have been done [16–18]. Rostamiyan et al. [16] investigated the microstructure and mechanical properties of 6061 aluminum alloy conventional FSSW and UAFSSW joints. Liu et al. [17] and Shi et al. [18] reported the material flow behavior of UAFSW and discovered that the material flow behavior was evidently enhanced during UAFSW. However, studies about UAFSSW of magnesium to aluminum alloys have not been reported yet. Therefore, in the present study, UAFSSW was applied to weld Mg alloy and Al alloy. Effects of ultrasonic vibration on hook defect, SZ width, microstructure of the joints, distribution of the IMC and fracture paths were studied in detail.

Experiment Process. AZ31B magnesium alloy and 6061-T6 aluminum alloy were used as the base material (BM) in the present study. Dimensions and configuration of the two sheets are indicated in Fig. 1. Prior to welding, all sheets were cleaned with sand paper to clean off the oxidation layer. The rotating tool was composed of a concentric shoulder and a tapered pin. The diameter of the shoulder is 11 mm and the pin has a right-hand threaded. Diameters of the pin root and bottom are 5 to 3 mm, respectively. The FSW-3LM-4012 machine was used in the experiment. The tool rotated in an anti-clockwise direction and the tilted angle is 0° . Ultrasonic vibration was exerted 5 s before the plunge of the pin and it was exerted on the lower plate under the SZ, as shown in Fig. 1. The vibration frequency was 19 kHz. Pin rotating speed and dwell time were 1000 rpm and 5 s. Other parameters such as plunge speed, shoulder plunge depth, and retracting speed are 5 mm/min, 0.3 mm, and 10 mm/min, respectively. After the retraction of the pin, the ultrasonic vibration lasted for another 5 s.

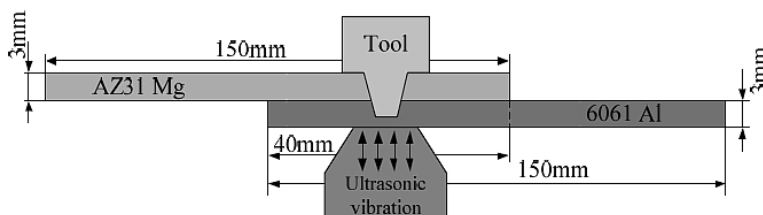


Fig. 1. A schematic illustration of the ultrasonic vibration during welding.

After welding, the metallographic specimens were cut through the center of the joint using a wire electrical discharge cutting machine. Then the specimens were burnished, polished and etched with Keller's reagent. Metallographic analysis was carried out using an optical microscopy (OLYMPUS-G71). Fracture positions of the specimens were observed using a stereoscopic microscope (ZSA403). The IMC composition was examined using a SU3500 scanning electron microscope (SEM) with energy dispersive X-ray spectroscopy (EDX) capabilities.

Results and Discussion. Cross sections of conventional FSSW and UAFSSW joints are shown in Fig. 2. It can be seen that in the SZ, 6061 Al alloy flows upwards and mixes with the AZ31 alloy due to the rotation of the tool. An up-bending interface exists between the AZ31 Mg alloy and the 6061 Al alloy, which is called the hook defect. According to Yin et al. [9], the geometry of the hook defect largely influenced the lap shear failure of the joint and better mechanical properties were attained when the hook height was small. As shown in Fig. 2a, 6061 Al alloy not only flows upwards into the upper sheet but also flows outwards. Hence, hook defect of the conventional FSSW joints curved outwards from the axis of the rotating pin. In the UAFSSW joints in Fig. 2b, 6061 Al of the lower sheet mainly shows upward flow and the hook defect is flatter.

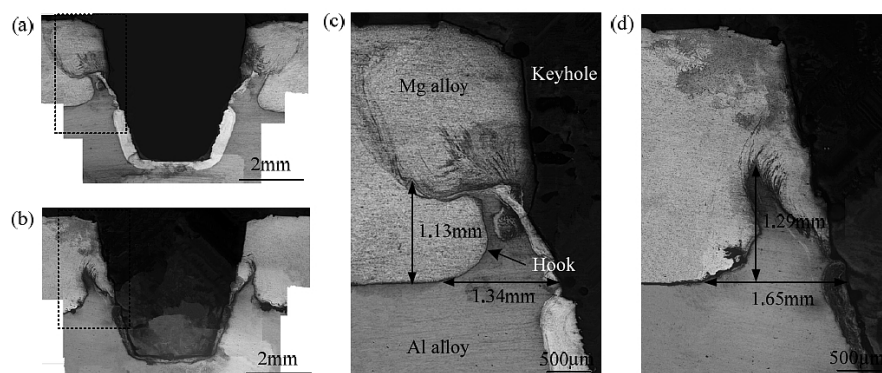


Fig. 2. Cross sections of the FSSW joints: (a) conventional FSSW joint; (b) UAFSSW joint; (c) magnified view of the region marked (a); (d) magnified view of the region marked (b).

The SZ width refers to the width from the origin of the hook defect to the keyhole. As shown in Fig. 2, SZ width is 1.34 mm of conventional FSSW joint while this width of the UAFSSW joint is 1.65 mm. The maximum flow distance of Al alloy on the conventional FSSW and UAFSSW tool is 1.13 and 1.29 mm, respectively. The results agree with the conclusion of Shi et al. [18]. During the UAFSSW process, the material flow behavior of the SZ is enhanced due to the ultrasonic vibration, which means more material adjacent the original SZ will be driven to flow. Therefore, the enhanced material flow behavior is beneficial to the upward flow of the lower 6061 Al alloy, as shown in Fig. 2b.

As shown in Fig. 3, at the end section of the hook defect, mixing degrees between the two materials show much difference. On conventional FSSW joint, mixing degree between 6061 Al and AZ31 Mg is not so adequate and the intersection where IMC always appear can be clearly recognized. Better mixing is formed on UAFSSW joint. As shown in Fig. 3b, plenty of complex lamellar-like shear bands formed between 6061 Al alloy and AZ31 Mg alloy. Therefore, the conclusion can be attained that ultrasonic vibration can enhance material mixing when welding dissimilar alloys.

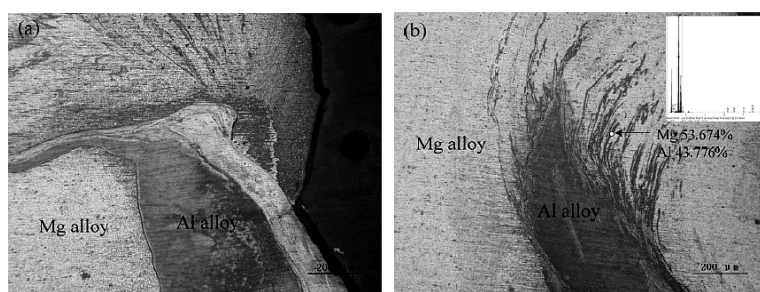


Fig. 3. Mixing of the dissimilar materials on two different joints: (a) conventional FSSW joint; (b) UAFSSW joint.

In FSW, the microstructure of the SZ plays a predominant part on joints quality. In general, uniform and fine grains of the SZ always results in better strength and higher hardness. On the contrary, non-uniform grains of the SZ leads to poor joint strength. The grains of the SZ on the conventional FSSW joint and UAFSSW joint are shown in Fig. 4. It can be seen that compared with grains shown in Fig. 4a, uniform and finer grains are observed on the UAFSSW joint. During the UAFSSW process, the fluidity of material is evidently enhanced due to the ultrasonic vibration. Higher flow velocity is beneficial for the strain and strain rate of the material in SZ, which is beneficial to the dynamic

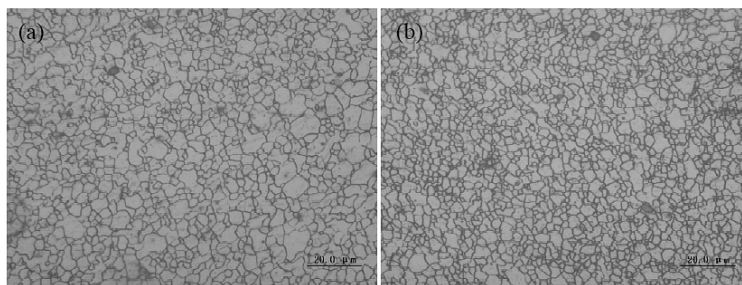


Fig. 4. Grains in the SZ on two different joints: (a) conventional FSSW joint; (b) UAFSSW joint.

recrystallization. Therefore, finer grains are attained in the SZ of the UAFSSW joint. As shown in Fig. 4, the average size of the grains decreases from 8 to 4 μm when the UAFSSW is used.

Fracture positions of the conventional FSSW joints and UAFSSW joints are shown in Fig. 5. It can be seen that both joint fracture at the hook defect firstly. When it comes to the region adjacent to the keyhole, crack propagation path shows difference. As shown in Fig. 5a, in conventional FSSW joint, crack propagates exactly along the interface between the two materials and presents an inverted “V” shape. On the UAFSSW joint, after initiating at the tip of the hook, the crack propagates along the hook and then upwards. At the region adjacent to the keyhole, crack shows a flat fracture path towards the keyhole instead of exactly along the interface. A portion of Mg alloy remains at the lower Al alloy, as shown in Fig. 5e and 5f.

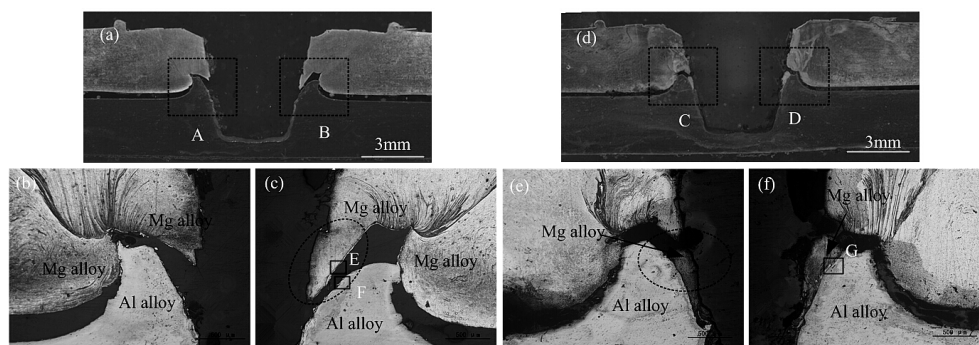


Fig. 5. Fracture positions of the joints: (a) general view of the conventional FSSW joint; (b) magnified view of the region A; (c) magnified view of the region B; (d) general view of the UAFSSW joint; (e) magnified view of the region C; (f) magnified view of the region D.

Figures 6 and 7 show the SEM images and the EDX analysis results of the region E, F, and G marked in Fig. 5. As shown in Fig. 6a, the main component of the IMC is 47.329% Mg and 51.246% Al at the Mg side. While at the Al side, the IMCs are mainly composed of 32.037% Mg and 64.637% Al. Therefore, it is believed that on the lap interface of conventional FSSW joints, the Al_3Mg_2 is the main component of the IMC. As shown in Fig. 7, region B locates at the interface between the two dissimilar alloys. The main components of the IMC are 53.464% Mg and 43.484% Al. It can be seen the percentage of the Mg is much bigger than that on the conventional FSSW joint. Possible reason for this is that when the ultrasonic vibration was used, material flow behavior at the lap interface was evidently enhanced. The mixing degree between the two materials becomes better on the UAFSSW joint, leading to an average elemental composition. It is believed on the UAFSSW joints, $\text{Al}_{12}\text{Mg}_{17}$ is the main component of the IMC.

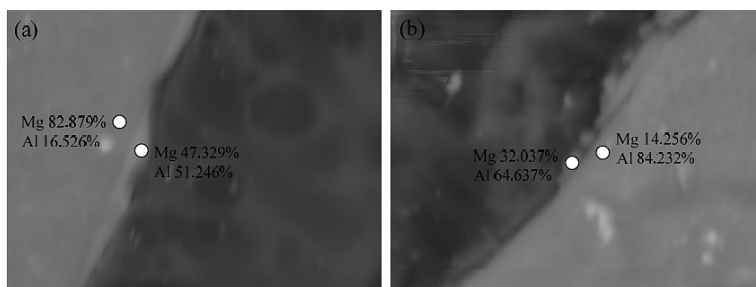


Fig. 6. EDX results on the conventional FSSW joint: (a) region E; (b) region F.

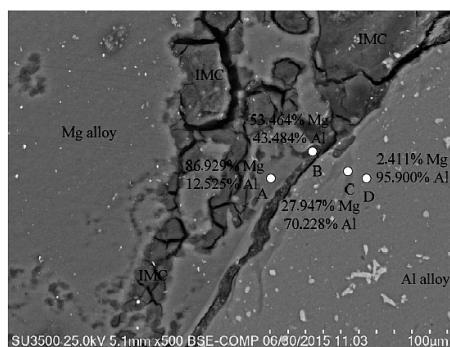


Fig. 7. EDX results of region G on the UAFSSW joint.

Conclusions. In the present study, UAFSSW was used to weld dissimilar Mg alloy and Al alloy, effects of ultrasonic vibration on the material flow, mixing degree, SZ grains and fracture modes of the conventional FSSW and UAFSSW joints were studied. The following conclusions can be drawn:

1. Ultrasonic vibration is beneficial for the upward flow of the lower sheet material. The upward flow distance and width of SZ on the UAFSSW joint are much bigger than those on the conventional FSSW joint. The mixing degree of the dissimilar materials is much better when ultrasonic vibration is used.

2. The grain size of the SZ on the UAFSSW joint is smaller than that on the conventional FSSW joint because of the ultrasonic vibration.

3. On the conventional FSSW joint, crack exactly propagates along the faying interface of dissimilar materials. On the UAFSSW joint at the region adjacent to the keyhole, crack shows a flat fracture path towards the keyhole instead of exactly along the interface, leaving a portion of Mg alloy at the lower Al alloy.

4. The main component of the IMC at the lap interface on the conventional FSSW joint is Al_3Mg_2 and the main component of the IMC at the lap interface on the UAFSSW joint is $Al_{12}Mg_{17}$.

Acknowledgments. This work is supported by the National Natural Science Foundation of China (No. 51204111), the Education Department Foundation of Liaoning Province (Nos. LJQ2012015 and L2012047), the Natural Science Foundation of Liaoning Province (No. 2013024004) and the Project of Science and Technology Department of Liaoning Province (No. 2013222007).

1. Y. H. Yin, A. Ikuta, and T. H. North, "Microstructural features and mechanical properties of AM60 and AZ31 friction stir spot welds," *Mater. Des.*, **31**, 4764–4776 (2010).

2. H. Badarinarayan, Y. Shi, X. Li, and K. Okamoto, "Effect of tool geometry on hook formation and static strength of friction stir spot welded aluminum 5754-O sheets," *Int. J. Mach. Tool. Manuf.*, **49**, 814–823 (2009).
3. R. Z. Xu, D. R. Ni, Q. Yang, et al., "Influencing mechanism of Zn interlayer addition on hook defects of friction stir spot welded Mg–Al–Zn alloy joints," *Mater. Des.*, **69**, 163–169 (2015).
4. Z. H. Zhang, X. Q. Yang, J. L. Zhang, et al., "Effect of welding parameters on microstructure and mechanical properties of friction stir spot welded 5052 aluminum alloy," *Mater. Des.*, **32**, 4461–4470 (2011).
5. W. Y. Li, J. F. Li, Z. H. Zhang, et al., "Improving mechanical properties of pinless friction stir spot welded joints by eliminating hook defect," *Mater. Des.*, **62**, 247–254 (2014).
6. S. Babu, G. D. Janaki Ram, P. V. Venkitakrishnan, et al., "Microstructure and mechanical properties of friction stir lap welded aluminum alloy AA2014," *J. Mater. Sci. Technol.*, **28**, No. 5, 414–426 (2012).
7. Y. C. Chen and K. Nakata, "Friction stir lap joining aluminum and magnesium alloys," *Scripta Mater.*, **58**, 433–436 (2008).
8. R. Cao, Q. Huang, J. H. Chen, and P. C. Wang, "Cold metal transfer spot plug welding of AA6061-T6 to galvanized steel for automotive applications," *J. Alloys Compd.*, **585**, 622–632 (2014).
9. Y. H. Yin, N. Sun, T. H. North, and S. S. Hu, "Influence of tool design on mechanical properties of AZ31 friction stir spot welds," *Sci. Technol. Weld. Join.*, **15**, No. 1, 81–86 (2010).
10. S. Bozzi, A. L. Helbert-Etter, T. Baudin, et al., "Influence of FSSW parameters on fracture mechanisms of 5182 aluminum welds," *J. Mater. Process. Technol.*, **210**, 1429–1435 (2010).
11. S. O. Yoon, M. S. Kang, Y. J. Kwon, et al., "Influences of tool plunge speed and tool plunge depth on friction spot joining of AA5454-O aluminum alloy plates with different thicknesses," *Trans. Nonferrous Met. Soc. China*, **22**, s629–s633 (2012).
12. V. X. Tran, J. Pan, and T. Pan, "Fatigue behavior of aluminum 5754-O and 6111-T4 spot friction welds in lap-shear specimens," *Int. J. Fatigue*, **30**, 2175–2190 (2008).
13. H. M. Rao, W. Yuan, and H. Badarinarayan, "Effect of process parameters on mechanical properties of friction stir spot welded magnesium to aluminum alloys," *Mater. Des.*, **66**, 235–245 (2015).
14. P. C. Lin, Z. M. Su, R. Y. He, and Z. L. Lin, "Failure modes and fatigue life estimations of spot friction welds in cross-tension specimens of aluminum 6061-T6 sheets," *Int. J. Fatigue*, **38**, 25–35 (2012).
15. Y. S. Sato, A. Shiota, H. Kokawa, et al., "Effect of interfacial microstructure on lap shear strength of friction stir spot weld of aluminum alloy to magnesium alloy," *Sci. Technol. Weld. Join.*, **15**, No. 4, 319–324 (2010).
16. Y. Rostamiyan, A. Seidanloo, H. Sohrabpoor, and R. Teimouri, "Experimental studies on ultrasonically assisted friction stir spot welding of AA6061," *Arch. Civ. Mech. Eng.*, **15**, 335–346 (2015).
17. X. C. Liu and C. S. Wu, "Material flow in ultrasonic vibration enhanced friction stir welding," *J. Mater. Process. Technol.*, **225**, 32–44 (2015).
18. L. Shi, C. S. Wu, and X. C. Liu, "Modeling the effects of ultrasonic vibration on friction stir welding," *J. Mater. Process. Technol.*, **222**, 91–102 (2015).

Received 03. 08. 2015